COBE-PREPRINT-NO-93-10F
C93/07/11-2

Fermilab Library
0 1160 0020718 7

INVESTIGATION OF THE ZODIACAL LIGHT FROM 1 TO 240 μm USING COBE DIRBE DATA

Micrometers

Thomas Kelsall[1], Michael G. Hauser[1], G.Bruce Berriman[2], Nancy W. Boggess[1], S.Harvey Moseley[1], Thomas L. Murdock[3], Robert F. Silverberg[1], William J. Spiesman[2], Janet L. Weiland[2]

[1]NASA Goddard Space Flight Center, Code 685, Laboratory for Astronomy and Solar Physics, Greenbelt, MD 20771
[2]General Sciences Corporation, Code 685.3, NASA Goddard Space Flight Center, Greenbelt, MD, 20771
[3]General Research Corporation, 5 Cherry Hill Drive, Danvers, MA 01923

COBE-Preprint NO-93-10F

ABSTRACT

The Cosmic Background Explorer (COBE) satellite was launched on 18 November 1989 from Vandenberg Air Force base on a Delta rocket. It carried two superfluid liquid-helium-cooled (LHe) infrared (IR) instruments in a 600 liter dewar, and three microwave radiometers mounted on the outside of the dewar. One of the LHe-cooled instruments is a ten-band photometer covering the spectral range from 1.2 to 240 μm -- the Diffuse Infrared Background Experiment (DIRBE). A goal of the DIRBE program is to obtain full-sky infrared observations that can be used to model accurately the IR contributions arising from the interplanetary dust (IPD) and the Galaxy. Using such models, the foreground can be removed to expose an underlying extragalactic IR component produced early in formation of the universe. The nature of the IPD IR foreground detected by the DIRBE is found to be quite complex, but amenable to modelling.

1. INTRODUCTION

The primary goal of the DIRBE program is the detection of IR signatures of the early formation of proto-galaxies and galaxies in the universe - the cosmic infrared background (CIRB)[1]. But to reveal the faint isotropic CIRB it is essential to obtain the highest accuracy data on the IR foreground contributions from the IPD and from our Milky Way Galaxy. Using these measurements as a basis for constructing models of these foregrounds, we believe it is possible to effectively remove them from the survey maps and disclose the CIRB. This is an intricate enterprise as the CIRB is estimated to be only a few percent or less of the IR emissions from the sky. There are, however, two "windows" where the contributions from these foregrounds is least -- around 3.5 microns and 200 microns. It is hoped that our modelling efforts will have the requisite precision to remove the contaminating foregrounds and to permit a measurement of, or the setting of stringent upper limits on, the CIRB. The overall COBE mission and the instruments have been described by Boggess et al.[2] and Mather[3].

The effects of the IPD scattering Sun light, the zodiacal light and gegenschien, have been studied extensively in the visible. More recently, IR investigations have been carried out, for example, under the ZIP program in the near to mid IR (2-35 μm) wavelengths using rocket-borne photometers [4-5]. In 1983 a full-sky, four-band, 12-to-100 micron survey was performed using the Infrared Astronomical Satellite (IRAS)[6-8]. The DIRBE program extends these researches by providing a full-sky survey in ten bands from 1.2 to 240 μm. As a valuable adjunct to the study of the IR sky brightness, the linear polarization in the 1.2-to-3.5 μm region also is measured as a delineator of the nature of the IPD. The DIRBE survey, which is the basis for this presentation, was executed between 11 December 1989 to 21 September 1990, when the instrument was cryogenically cooled. Data of reduced sensitivity continue to be collected in the four shortest wavelength bands (1.2-4.9 μm) which use InSb detectors. These later data will be valuable in further study of the parameters defining the IPD.

In order to detect the light from the IPD in an unambiguous manner, the DIRBE is mounted at 30 degrees to the spin axis of the COBE, which rotates at 1 revolution each 72 seconds. The 30 degree cant makes the DIRBE execute a helical track on the sky as the COBE spins and moves about its orbit. With a half-angle of 30 degrees, the viewing swath enclosing this track covers one half of the sky. But this portion of the sky is not fully sampled in a single orbit, as the field of view (FOV) of the DIRBE is only 0.7 degree, while the COBE moves at about 3.5 degrees/minute in its 103-minute-period orbit. In about ten orbits, one half the sky is fully sampled. This viewing strategy provides a modulation of the IPD signal as the solar elongation angle for an observation of any celestial sky pixel varies in time (60 days at the ecliptic equator) from about 64 degrees to 124 degrees. Above the ecliptic latitude of 60 degrees the amplitude of the full swing in elongation drops off at about two degrees per degree of latitude, and is zero directly at the ecliptic poles. The coverage of the range in elongation is very dense as each pixel (0.32 × 0.32°; 393216 pixels on the whole sky) is seen on the average 2.4 times per day. But this average does not represent the time-dependent nature of the observations. The highest density of observations occur along

the edges of the viewing swath, and the least density at the center of the swath. Over the mission, the number of high-quality observations per pixel ranges from about 200 at the ecliptic equator to 800 near the ecliptic poles. A plot of the one-orbit-long track of the center of the FOV on an ecliptic coordinate view of the sky is shown in Fig. 1.1. As the COBE is in a Sun-synchronous polar orbit which precesses one degree per day, the whole sky is well sampled in half a year.

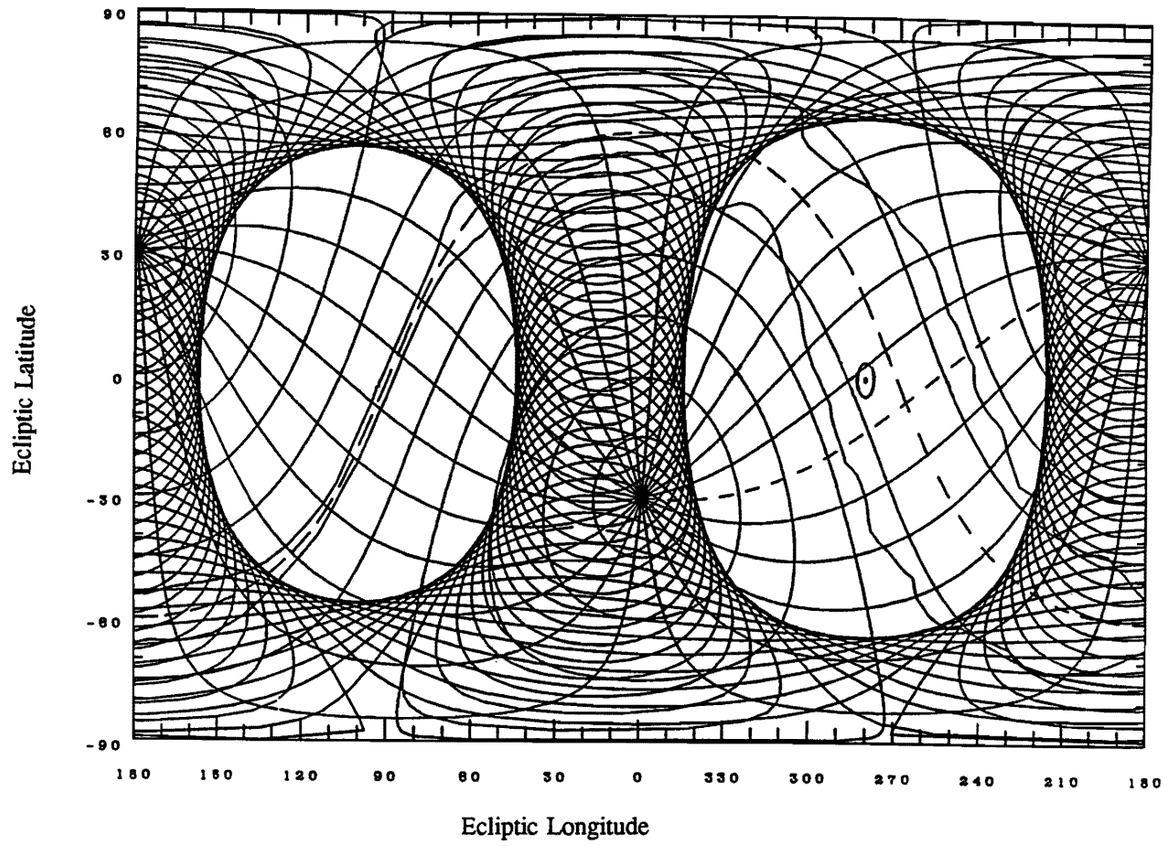

Fig. 1.1: The track of the DIRBE line of sight on the sky over the course of one orbit on 1 January 1990. The sky is presented in ecliptic coordinates, with an overlay grid of Galactic coordinates. The contour lines surrounding the Galactic equator (long dashes) outline the rough appearance of the Milky Way.

Knowing that the CIRB would be elusive and that the contaminating foregrounds are bright drove the DIRBE design. To ensure that a measurement was not distorted by the sidelobe response, the DIRBE is a highly-baffled, off-axis, 19-cm diameter Gregorian telescope with multiple field stops. To further suppress the sidelobes a Lyot stop is employed to reduce the diffraction from the primary mirror. The use of the Lyot stop comes with the modest penalty of reducing the full aperture by only 5%. On the basis of modelling the system[9] it was found that the main culprits in producing a poor level of off-axis rejection are rough primary and secondary mirrors -- these were superpolished. The effects of these efforts along with the maintenance of a class 100 cleanliness level did obtain a superior instrument. In fact, the response to the Moon is barely discernable when it is some 6 degrees off axis, and it does not drive the detectors into saturation until it appears in the 0.7° FOV. This result is impressive, as the modelling efforts indicated that there would be Moon effects when it first begins to illuminate the edge of the primary mirror, which occurs when it is 28° off axis. To eliminate variations in the quality of the photometry that occur if different bands observe a spot on the sky at different times, the detector assemblies are placed at a pupil image - the image of the primary mirror illuminated by the sky - so they all see the same patch of sky simultaneously. The consequence of this solution is that the detectors can only sample a portion of the image of the primary mirror -- the eight bands from 1.2 to 100 microns have a geometrical thruput of about 10%, while the two longest wavelength bands (bolometers at 140 and 240 μm) each receive via double beamsplitters the full image of the primary to overcome their lesser sensitivities. In order to achieve an "absolute" photometer with good stability a 32 Hz tuning-fork chopper imposes a signal at each detector

which oscillates between that from the sky and that from a zero-flux reference -- a 1.8-2.0K cold surface interior to the DIRBE. A datum from each of the 16 detectors is received every eighth of a second, and it is the synchronously-demodulated output from 4 chopper cycles. To measure the instrumental offsets, a cold shutter can be moved to close off the sky input at the first field stop. To ensure short-term photometric stability, the DIRBE includes four small resistive sources within an integrating sphere -- the DIRBE internal reference system (IRS). A chosen source is heated up in a monotonic staircase manner by an on-board EPROM-stored sequence from LHe temperature to about 600K with a modest power load on the dewar. In order to inject the signal from a source, the output of the integrating sphere faces into a set of relay optics which illuminate the backside of the cold shutter. On the backside of the shutter is a figured optic. This optic forms with the main optics from the secondary mirror onwards a reasonable facsimile of a diffuse-object image at the detector assemblies. The highly attenuated output from an IRS source is bright enough to stimulate all of the bands, many from a zero-response level to saturation. Long-term relative photometric stability is obtained by monitoring a network of stable celestial discrete sources. The absolute calibration is determined from observations of a few selected celestial objects and planets with well-known fluxes. A more extensive discussion of the DIRBE instrument is given by Silverberg et al.[10].

We chose to have ten bands covering the wavelength range from 1.2 - 240 μm, since these would obtain the information needed to detect and allow the modelling and elimination of the foregrounds; and they cover the wavelength range where various theories indicated that the CIRB might appear. The long wavelength cut off was picked to prevent response to the 3K cosmic background radiation (CBR) -- an interfering background from very early times in the evolution of our universe! This wavelength is also long enough to provide spectral overlap with the COBE FIRAS instrument.

The shortest wavelength bands are essentially mimics of the ground-based J (1.2 μm), K (2.2 μm), L (3.5 μm), and M (4.9 μm) bands. They are "mimics" in the sense that we did not tailor their bandpasses to make things equivalent to the effects imposed by observing from the ground through an absorptive atmosphere. These choices also permit easy transformation of a great wealth of previous results onto the DIRBE photometric system, and vice versa. It was also known that a cosmological "window" might be in the neighborhood of 3.5 microns where the scattering of Sun light by the IPD and the thermal emission of the IPD are low. It was recognized that the removal of the zodiacal emissions would be very difficult. It is, in fact, mathematically impossible to determine a unique model for a surrounding dust cloud; only by going out of the cloud can a unique model be determined. To get as much information as possible on the problem of discerning the zodiacal light, it was decided to add to the three shortest wavelength bands (1.2, 2.2, 3.5 μm) ancillary channels that measure the level of linear polarization. In each of these three bands there are three detectors: one for the measurement of the full intensity and two additional detectors for the measurement of the polarization. One of these detectors has the polarizers mounted in front of it so the plane of polarization is parallel to the scanning motion and the other channel measures the polarization in a plane perpendicular to the scanning motion. The rejection ratios of the polarizers are in excess of one hundred.

The next four bands are as close as possible to the four IRAS bands at 12, 25, 60, and 100 microns. Again an argument for the selection is the ability to compare the results of another survey to ours. The last two bands at 140 and 240 μm are unique to the DIRBE program, though they are related to the two bands used in a balloon-borne survey of the Galactic plane[11].

As demonstration of the brightness of the IPD emissive foreground, Fig. 1.2 shows a preliminary grey-scale image of the sky at 12 microns. The image is in Galactic coordinates, so the IPD emission snakes across the projection in the form of an inverted bright "z" concentrated along the ecliptic plane.

2. DATA-PROCESSING SCENARIO

The software constructed to handle the data from the instrument is made up of a number of independent modules, or what we call "facilities". These facilities are concatenated into an operating unit called the "Project Pipeline" (PPL)[12]. The PPL ingests the data and processes them so as to remove the instrumental signatures, and then places the resulting observations into time-ordered archives and sky arrays. Work on some of those "signatures" is still continuing as we attempt to achieve a better rectification of the effects from non-linearities, particularly those seen in the 60 and 100 μm bands which use Ge:Ga detectors. On top of the PPL are all the scientific-analysis software modules. The major steps in the processing of the data to make them useful in scientific analyses are given in Table 2.1. All of the code in the PPL has been validated by a team of astronomers, which is a very effective filter since poorly processed data is their bane when they do their scientific investigations. The validation of the PPL is almost complete, as we prepare to release our first data product to the public in June, 1993 -- a complete view of the Milky Way in all ten bands for a solar elongation angle of 90 degrees.

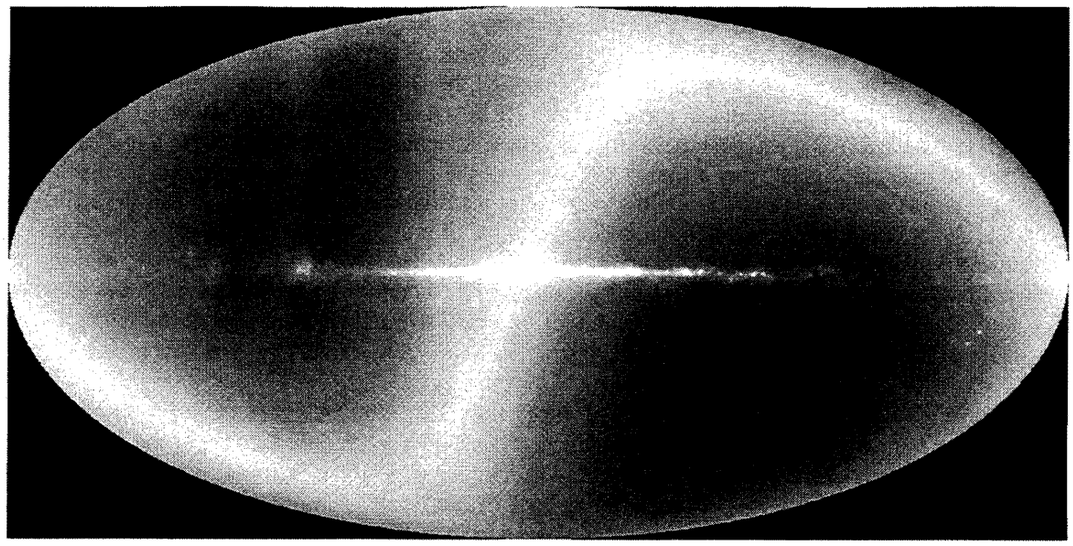

Fig. 1.2: The sky at 12 microns as it appears when the data are selected so the observation at each pixel is for a solar elongation angle of 90 degrees.

TABLE 2.1
SIMPLIFIED PRESENTATION OF THE DIRBE DATA PROCESSING BY THE PPL

DATA INGESTION: Accepts the data from the telemetry stream, removes all suspect data, and places them in a first time-ordered archive (TOA).
ARCHIVAL INDEX: Forms an index system that can be interrogated to determine when the instrument is in a specific state.
MERGE DATA: Adds to the TOA essential data on the operation of the spacecraft and the other instruments, orbital data, attitude, and the environment (e.g., in the South Atlantic Anomaly).
NOISE CHARACTERIZATION: Filters the time-ordered data, removes spikes formed by charged particles, and generates information on the glitch rate and the general character of the noise.
ENGINEERING TRENDS: Forms trends of all the engineering sensors.
RESPONSE TO INTERNAL CALIBRATORS: Tracks the responses of each detector to the IRS sources and to an electronic signal used to measure the gain of the analog electronics.
DETERMINATION OF GAIN CORRECTIONS: Finds from the response to the IRS the gain corrections to maintain short-term photometric stability.
LINEARIZATION OF THE OBSERVATIONS: Applies all corrections to the data needed for the removal of the instrument signature.
CAPTURE AND STUDY OF CELESTIAL OBJECTS: Detects the passages of discrete sources, evaluates their photometry, and separates out the time strings of the approved calibrators and the planets; the observations of the calibrators are used to determine long-term gain corrections.
STUDY OF THE BEAM RESPONSE PROFILE: Determines the near and far field stray light response and produces the beam profile.
CREATION OF DAILY SKY MAPS: Converts the TOA into a sky array where under each pixel are data on every observation and a set of ancillary information with each observation.
APPLICATION OF CELESTIAL-BASED CORRECTIONS: Applies the final gain corrections based on the sightings of stable celestial sources to each observation and, based on the study of the responses to planets and selected calibrators, modifies the data to place them on an absolute basis (MJy/sr).
FORMATION OF WEEKLY-AVERAGED SKY MAPS: Ingests the corrected daily sky maps and forms weekly-averaged results at each pixel.
SKY-MAP PRODUCTS: Provides special products such as the appearance of the sky for a particular time period or for a specific value of elongation (the sky for an elongation of 90° is one such product).

3. THE QUALITY OF THE DATA

The operation of the instrument is near flawless, and overall the noise of the sky observations is limited by the detector noise at low sky levels and photon and/or "confusion" noise at high sky levels in complex regions (e.g., the Galactic center). There are, however, a few quirks in the DIRBE performance which affect the data quality.

One anomaly is an InSb detector in one of the two 1.2 μm polarization channels that shows a highly variable gain and excessive noise. We refer to this phenomenon as "lunacy", as late in the mission it was found to be triggered by passages of the Moon. That channel is made to perform as well as the other InSb detectors by turning it off during those two times a month when the Moon is in the viewing swath. One of the Si:As-BIB detectors (25 μm band) shows a very low level trace (1-2%) of "lunacy". The data from both "lunatic" channels are returned to a stable base upon application of the gain corrections based on the observations of celestial calibrators. The heater mounted underneath the 100 μm Ge:Ga sensor did not operate, which meant the detector had to run colder than desired and the effects of gain-increases due to hits from trapped protons when going through the South Atlantic Anomaly could not be annealed away by increasing the sensor's temperature to about 20 K, as was done for the other Ge:Ga detector (60 μm). This detector was annealed by flooding the detector with a strong light from the IRS. An unexpected quirk is the photon-induced effect on the gain of the Si:As-BIB detectors and the Ge:Ga detectors, and this effect is initiated by the operation of our internal calibrator, the IRS. Finally, there are significant non-linearities (from a few to 20-30%) in the response of the Ge:Ga detectors. It is clear that no simple linear process can be applied to remove this behaviour. We are still studying methods for reducing the magnitude of these effects. However, for the observations of the IPD brightness, which is a smoothly varying function of direction in the viewing swath, most of these troubles can be made inconsequential by basing the study on selected patches where the anomalies are not in evidence.

The caliber of the data is represented in Fig. 3.1, where observations at 25 μm of two high ecliptic latitude pixels are shown. The bottom two panels in the presentation show the deviation of the observations with time about a harmonic fit to the variation of the IPD emission under the assumption of a period of one year, and the distribution of those deviations. The RMS of the deviations is only 1.5 times the shutter-closed, dark noise, and indicates a photometric precision of about 1% per observation. But as noted above, and as demonstrated in Fig. 3.1, the method of observing the sky means that some hundreds of observations are taken at each pixel, so that at even the faintest pixel the signal-to-noise ratio reaches a level of one hundred. Since the IPD light is smoothly varying, the nature of that variation in time and space can be specified to significantly higher relative accuracy.

4. EVIDENCE OF THE IPD SCATTERING AND EMISSION IN THE DATA

Upon first light in late November 1989 we quickly looked at the output of the channels measuring the polarization. We were satisfied to see that the time variation of the output showed a double sinusoidal behaviour as the COBE made one revolution. As expected from the IRAS results, even using the rawest form of the data the IPD thermal emission in the 12 and 25 micron bands dominated the sky, as shown in Fig. 1.2 for the 12 micron band.

One model-independent measure of the nature of the IPD cloud is provided by simply plotting the results at the ecliptic poles[13]. The observed sinusoidal oscillation of the IPD brightness at the poles immediately and directly indicates that the IPD cloud is inclined to the ecliptic plane[7,14-15]. The IRAS results showed that the plane is inclined at about 1.5 degrees. The behaviour at the poles for the 12 micron band is shown in Fig. 4.1.

The DIRBE data contain a wealth of information over the whole sky that better defines the symmetry of the IPD cloud. In Fig. 3.1 the upper two panels for each pixel show the observations versus time and the variation of the fit to those observations versus elongation. As can be seen the amplitude of the two pixels differ by 40%, and the variation with elongation is totally different. The signatures of the structure for the cloud persist to quite low values of ecliptic latitude. Fig. 4.2 shows the results for single pixels along the ecliptic longitude of 90 degrees at latitudes of -30, -13, -5, and 0 degrees. As can be seen, the end points at days 110 and 240 are both for elongations of 64 degrees, but the values of those end points are distinctly different, with that difference diminishing to near zero upon reaching the ecliptic equator. The set of clues as to the nature of the IPD cloud is being used to select best quasi-physical-model defining parameters (e.g., a modified fan model[16-17]).

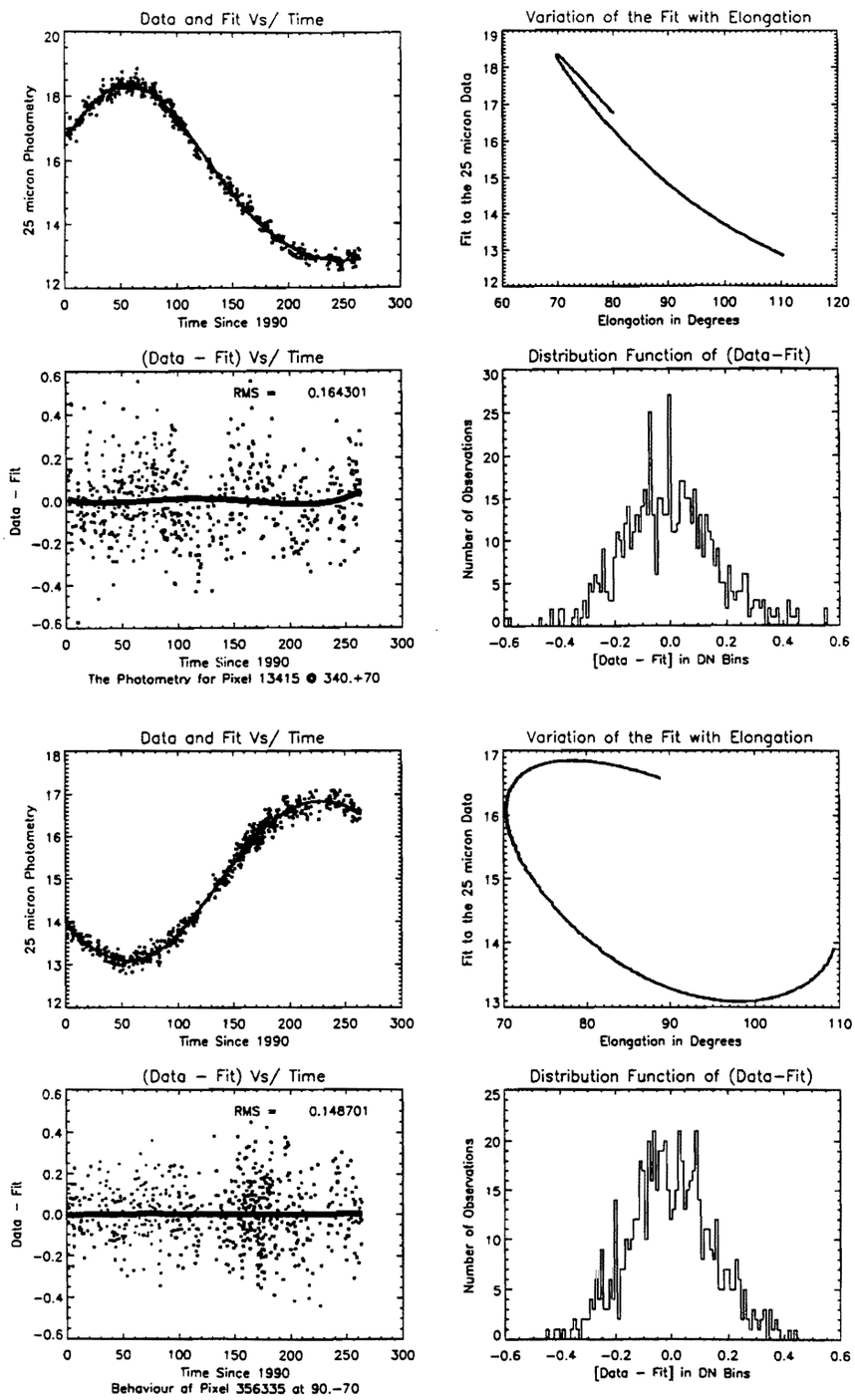

Fig. 3.1: The 25-micron observations (in data numbers) and fits for two high-latitude pixels: one at ecliptic coordinates of 340 and +70 degrees, and the other at 90 and -70 degrees. In each set of four panels, the left top panel shows the data and a harmonic fit; the right top panel shows the variation of the fit with elongation angle; the bottom left panel shows the residuals around the fitting curve and a fit to these residuals; and, the bottom right panel shows the distribution of these residuals.

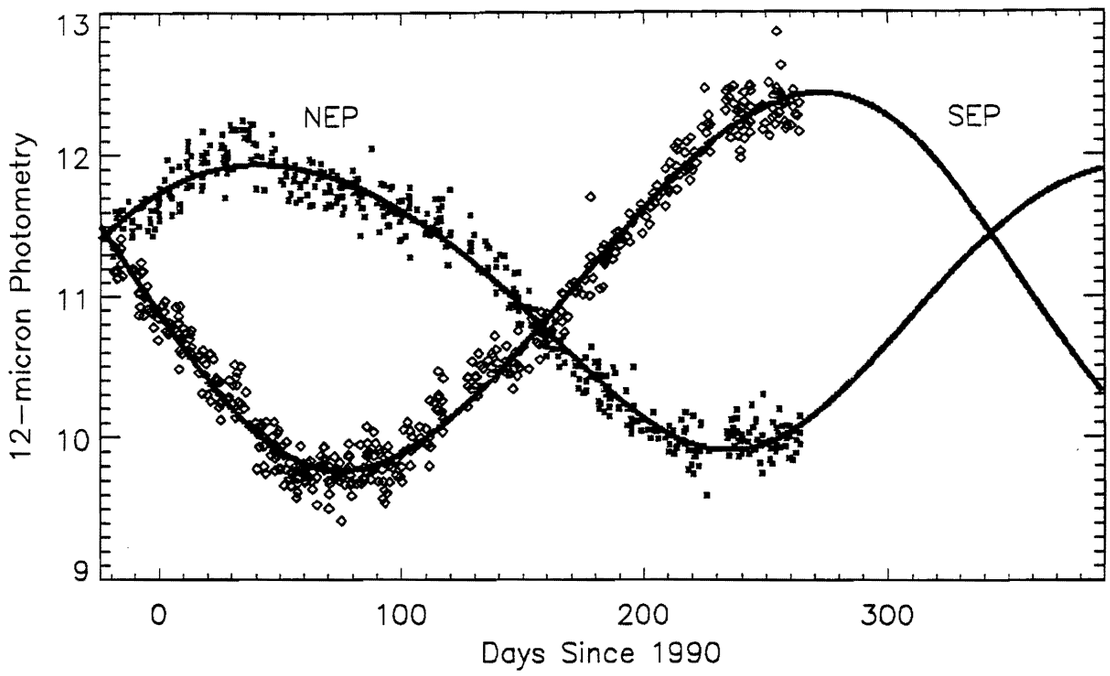

Fig. 4.1: The observations (in data numbers) and fits to the seasonal variation in the 12-micron photometry of one pixel at each of the ecliptic poles.

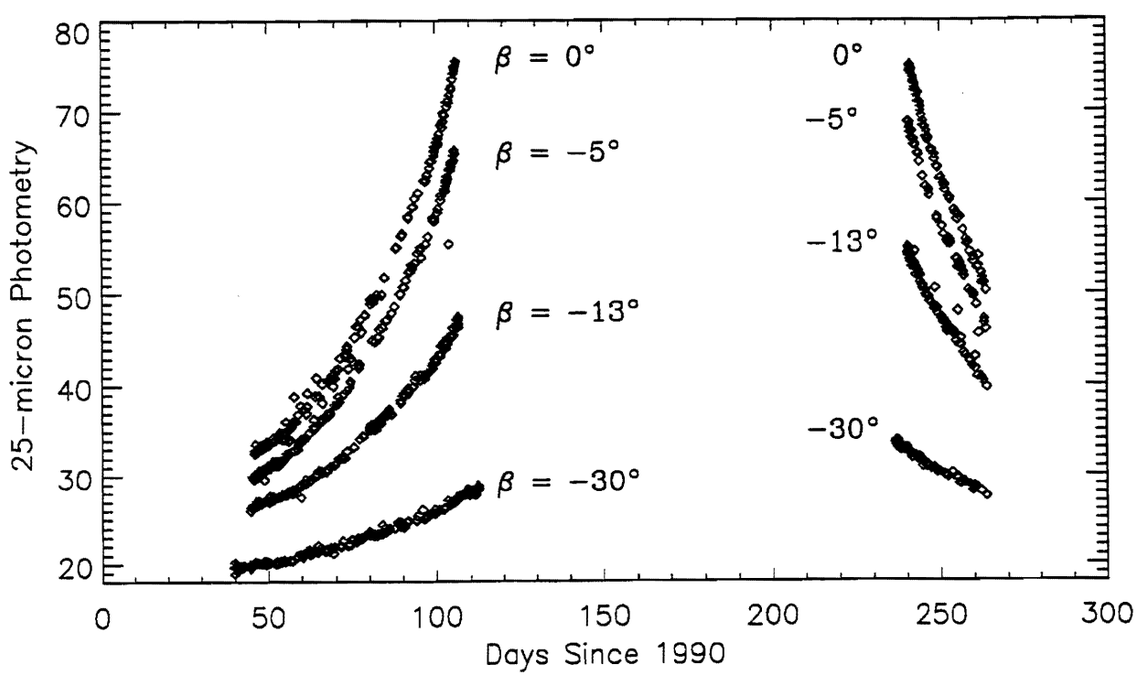

Fig. 4.2: The variation of response at single pixels along the ecliptic longitude of 90 degrees for four latitudes, as these pixels enter/transit/exit/re-enter the viewing swath. The first sighting around day 40 happens when the elongation is 124 degrees. The end points at around day 110 and the re-entering points around day 240 are both for an elongation angle of 64 degrees.

5. AN EMPIRICAL FITTING SCHEME

Our first attempt at extensively modelling the IPD signal is via the application of a phenomenological fitting function to the data. The function employed is one proposed by Hauser[5,18]. The form of the equation is given in eq. 5.1:

$$I=I_o-\kappa\{1-\beta_c|csc(\beta-\beta_o)|[1-\exp(-\chi-\alpha\chi^2)]\}, \qquad (5.1)$$

where I_o = peak intensity, β_o = ecliptic latitude at maximum intensity, β_c = width paremeter of the IPD brightness profile, κ = intensity scale factor which defines the plane-to-pole intensity contrast, $\chi = |(\beta-\beta_o)/\beta_c|$, and α = a parametric value chosen to minimize the residuals. The rationale behind the function is based on the requirements that the brightness variation follow a cosecant law at high latitudes as appropriate for a plane parallel structure of the IPD, and look like that from a disk of finite radius at low latitudes. This fitting equation was first applied to the IRAS data with good results. Other fitting equations have been proposed, also based on the IRAS data[19-21].

As the use of Eq. 5.1 is a phenomenological scheme, the method of application is to adjust the fitting parameters so as to reproduce a sensible lower envelope to the run of the brightness along a line of constant ecliptic longitude. An example of the data and a fit are shown in left panel of Fig. 5.1, and the residuals from the fit are shown in the right panel. Note in the residuals that the IPD bands, which were first detected by the IRAS scientists[8], are clearly visible. The bands are the presumed evidence of asteroidal collision[22-24]. These features are not built into Eq. 5.1, though they can be. The bands are very faint increments to the IPD brightness, being only about a few percent enhancement over the main IPD component near the equator (see Section 6).

To produce a fit for the whole sky, the first step is to interpolate the DIRBE results at each pixel to the first epoch when the solar elongation angle is 90 degrees. The conversion of the data over the whole sky to a single value of the elongation angle is done to avoid sudden discontinuities in the maps due to different solar elongations for adjacent regions, and because the empirical fitting function was designed on the basis of studying 90° elongation data from the IRAS survey. It is found, however, that the equation can be applied to data with any value of elongation. Operationally, the equation is used to construct fits at a set of ecliptic longitudes -- one for each 10 degrees in longitude. These 36 columns in a sky array can then be used to produce an answer at any latitude and longitude by bilinear interpolation. The results from a preliminary application of this approach, for the eight DIRBE bands from 1.2 - 100 microns, produce residual maps which are essentially free of the IPD foreground. The IPD bands stand out clearly. There are, however, also obvious artifacts from the subtraction process, but these appear only at levels similar to those of the bands; i.e., a few percent of the peak brightness at the equator. We are quite confident that with a second generation of processed DIRBE data and our experience with Eq. 5.1 that we can achieve consistent identification of the IPD signal to a few percent of the peak IPD brightness.

6. THE IPD BANDS

As noted, the banded structure in the zodiacal emission was first discerned in the IRAS data[8]. The bands are seen as symmetric pairings of enhanced brightnesses on either side of the ecliptic equator. In the IRAS data 3, and perhaps 4, pairs are found at ±1.4°, ±10°, and ±17° in ecliptic latitude. Their origins have been linked to asteroid-asteroid collisions of members of the Koronis, Themis, and Eos families of asteroids; with a less certain band associated with the Maria family[8,22-24]. The lower resolution maps created by DIRBE presently only show evidence of the bands at ±1.4 and ± 10°.

Though a variety of techniques have been used to uncover the bands in the IRAS data[22,24-25], we apply a yet different approach[26] to disclose the bands in the DIRBE weekly-averaged data. The basic ingredient in the method is to extract from the DIRBE data set only those observations which show a minimum-signal level -- i.e., show the lowest combination of brightnesses from all contributing emissions. To carry out this selection, the data are arranged in a grid of elongation and ecliptic latitude, which is believed to be sufficient based on the IRAS finding that the bands are nearly uniform in structure at all ecliptic longitudes. Then at each grid point, only that minimum datum per wavelength during the many weeks of the mission is selected as representative of the sky. The time of minimum is or can be, of course, wavelength dependent. This technique has the advantages of avoiding the difficulties associated with trying to filter out stellar sources in the time or spatial domain, and of removing the necessity to make assumptions about the underlying smooth component of the IPD signal.

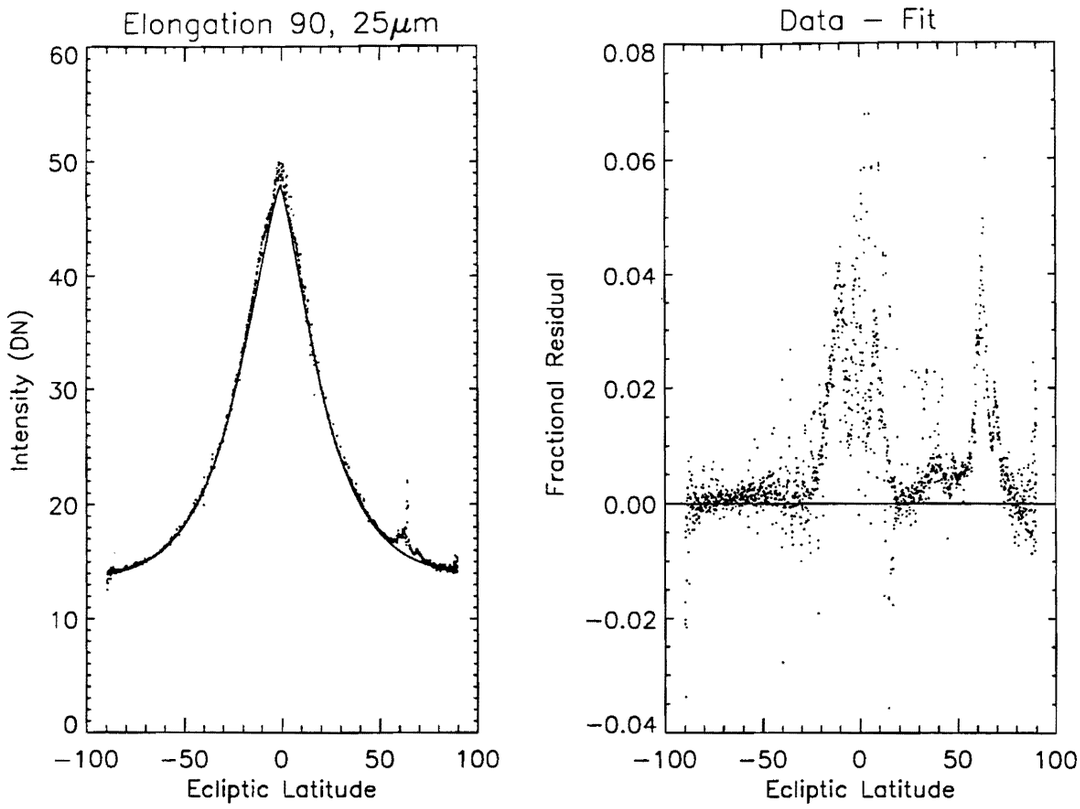

Fig. 5.1: The application of the empirical fitting function of Eq. 5.1. The left panel shows the 25-micron photometry (in data numbers) along the pole-to-pole path for the ecliptic longitude of 10 degrees. The data have been selected so each observation is for a solar elongation angle of 90 degrees. The solid line is the fit determined by adjusting the parameters of Eq. 5.1. The right panel shows the residuals, observations-fit, normalized to the peak value of the fit.

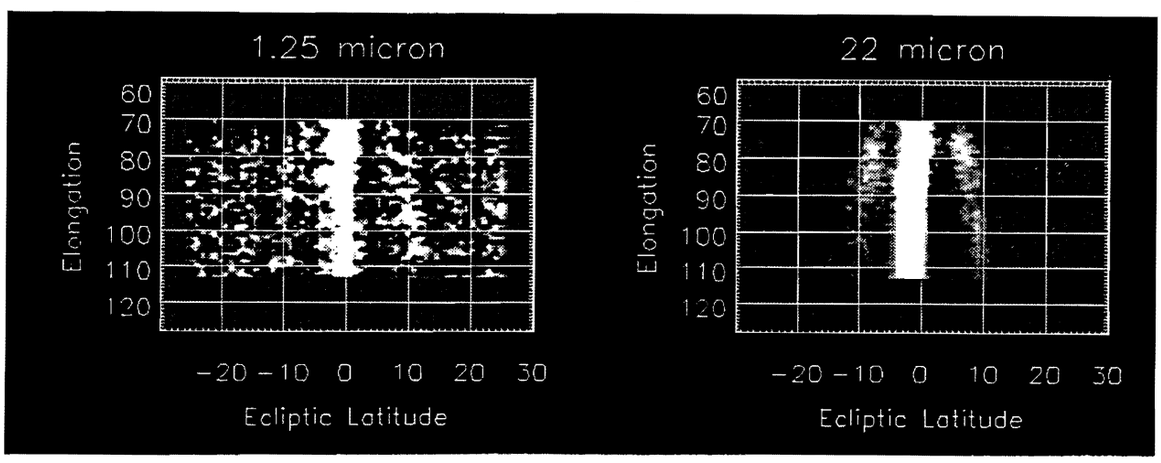

Fig. 6.1: Grey-scale images formed using the 1.2 and 22 micron observations of a section of the sky presented in ecliptic latitude and solar elongation angles to show the presence of the IPD dust bands.

The results from this study of the bands are shown by the representative grey-scale surface plots for 1.2 and 25 μm in Fig. 6.1. The DIRBE results extend the findings from the IRAS program, as we see evidence of the bands in emission at the IRAS wavelengths and in scattered light in the shorter wavelength bands. An analysis of the apparent separation of the bands as a function of elongation angle show parallactic distances of 2 and 1.3 AU for the 10 deg and 1.4 deg bands, respectively.

7. THE LEVEL OF POLARIZATION

As already noted, the DIRBE contains three wavelength channels (1.2, 2.2, and 3.5 μm) which measure both intensity and linear polarization. The method for measuring the state of polarization is unusual in order to avoid the additional costs and risks associated with incorporating a moveable analyzer which must work reliably at 1.5K. A static solution is employed where two additional detectors per band are installed, and these view the sky through fixed linear polarizers[27]. This is a simple optical-mechanical configuration, but it is limited in its returns because the full specification of the linear polarization is not possible at any one time for all pixels within the viewing swath. This limitation is the result of the fact that any pixel in the swath is swept across by the DIRBE in a restricted manner -- along the edges of the swath the transit path lies along a north-to-south or a south-to-north path; in the middle of the swath there are two transit paths which go from east-to-west or west-to-east; and, for all other points in the swath the transition between these extremes is a slowly varying function with position. However, as time passes and the orbit precesses, a polarization map of the full sky is generated.

In the data, the twice-per-spacecraft-rotation signature of linear polarization is strongly obvious, as is shown in Fig. 7.1. The magnitude of the polarization is roughly 10%, and the orientation is, as was expected, perpendicular to the ecliptic plane. The polarization varies only slowly from the plane to the pole. The precision of the polarization measurement is limited by sky noise due to the variable number of stars that are in the beam at any one instant. This sky noise changes on a given pixel

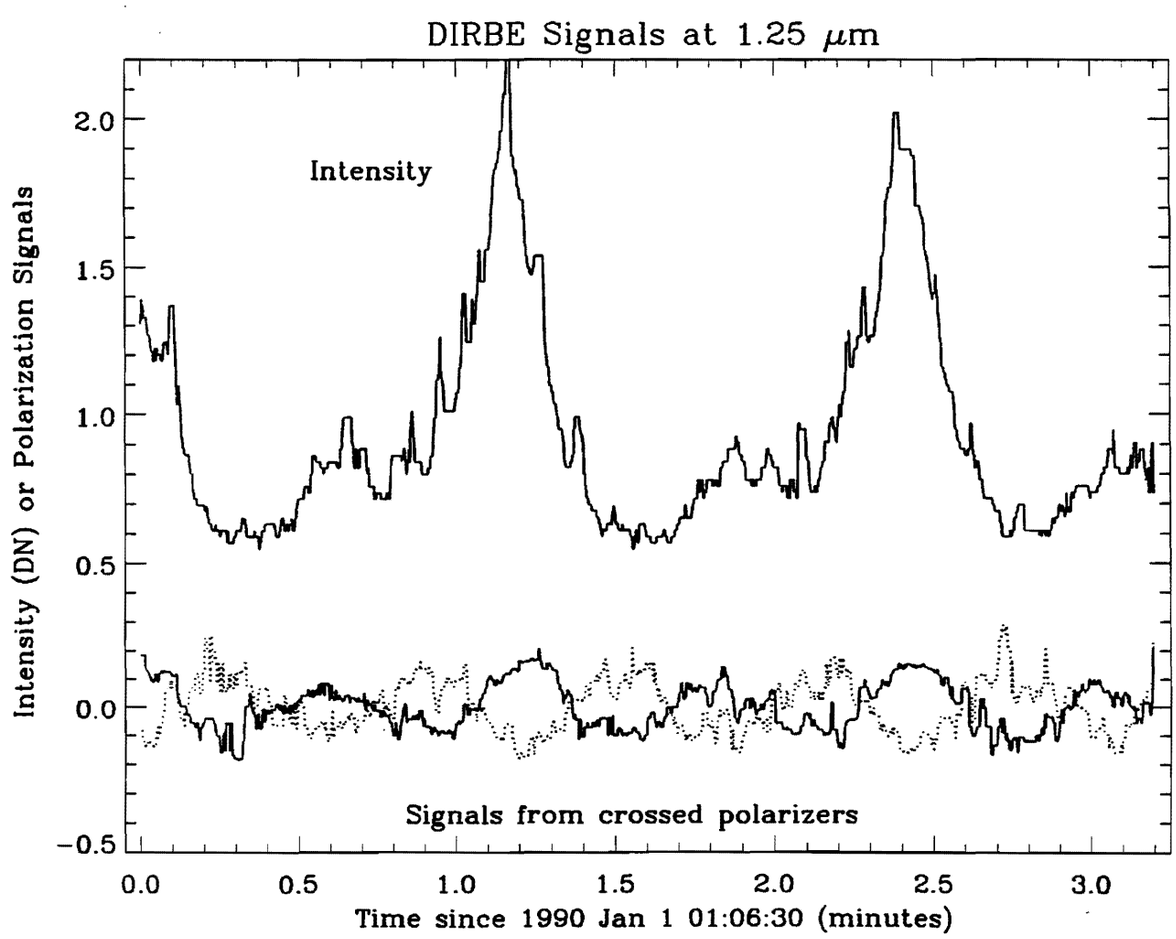

Fig. 7.1: The evidence of the polarization of the IPD brightness in the time-ordered 1.2 micron data over 2.7 revolutions of the COBE. The basic data have been smoothed with an 11-point running median filter. The top curve shows the output of the full-intensity channel (in data numbers), where a 3-to-1 variation in the IPD signal occurs upon each revolution of the COBE. The bottom two curves show the polarization signals[27] for each of the two polarization channels.

as the viewing swath moves across the sky since the approach to that pixel is along systematically varying paths across the sky. But one advantage of mounting the detectors at a pupil image is that this noise is correlated in the 3 detectors at each wavelength, and so tends to cancel when forming the ratios of their responses. The effects of the point sources can be further mitigated by applying a time or spatial filter to the data, or by simply choosing the least noisy pixels across the sky. We find quiet pixels even within a few degrees of the Galactic center, where the sky noise is severe. With some effort we can achieve a precision of the polarization measurements for 1-degree fields that approaches 1% or better.

8. SUMMARY

The DIRBE instrument and the viewing strategy employed to scan a range in elongation from 64 to 124 degrees is shown to be a powerful delineator of the sky brightness arising from the IPD. The DIRBE data base on the scattering and emission from the IPD covers at least 8 wavelengths spanning the interval from 1.2 to 100 microns. The zodiacal emission contribution to the 140 and 240 micron sky brightness is very small and is presently only tentatively detected. The IPD cloud appears more complex than simple symmetries that have been proposed, but the DIRBE data base contains the clues to determine the structure. Knowledge of the nature of the cloud will be furthered by the DIRBE measurements of the polarization in the J, K, and L bands. The enhanced features known as the IPD dust bands are visible from 1.2 to 100 micron wavelengths.

9. ACKNOWLEDGEMENTS

The DIRBE program required the efforts of many people. Their efforts have paid off with a handsome return of excellent data. We would here like to express our warm appreciation to the Drs. John Arthur Skard and Gary Toller and their colleagues who labored mightily to produce, test, and validate the data-reduction software and to process all of the DIRBE data using the PPL.

The COBE program is supported by Office of Space Science at NASA Headquarters. The Goddard Space Flight Center (NASA/GSFC) is responsible for the design, development, and operations of the COBE and its instruments; it is also responsible for the generation of the data-processing software and the production of all public data products. The NASA/GSFC is provided with scientific guidance by the COBE Science Working Group.

BIBLIOGRAPHY

[1] M.G. Hauser et al., "The Diffuse Infrared Background: COBE and Other Observations", "After the First Three Minutes" (eds: S.S. Holt, C.L. Bennett, and V. Trimble), AIP Conf. Proc., **222**, 161, 1991.

[2] N.W. Boggess et al., "The COBE Mission: Its Design and Performance Two Years After Launch", Astrophys. J., **397**, 420, 1992.

[3] J.C. Mather, this conference.

[4] T.L. Murdock and S.D. Price, "Infrared Measurements of the Zodiacal Light", Astron. J., **90**, 375, 1985.

[5] L.J. Rickard, S.W. Stemwedel, and S.D. Price, "Reconciling ZIP and IRAS Observations of the Zodiacal Background", "After the First Three Minutes" (eds: S.S. Holt, C.L. Bennett, and V. Trimble), AIP Conf. Proc., **222**, 183, 1991.

[6] G. Neugebauer et al., "The Infrared Astronomical Satellite (IRAS) Mission", Astrophys. J. Lett., **278**, L1, 1984.

[7] M.G. Hauser et al., "IRAS Observations of the Diffuse Infrared Background", Astrophys. J. Lett., **278**, L15, 1984.

[8] F.J. Low et al., "Infrared Cirrus: New Components ofthe Extended Infrared Mission", Astrophys. J. Lett., **278**, L19, 1984.

[9] D.C. Evans, "Principles of Stray Light Suppression and Conceptual Application to the Design of the Diffuse Infrared Background Experiment for NASA's Cosmic Background Explorer", SPIE Proc., **384**, 82, 1983.

[10] R.F. Silverberg et al., this conference.

[11] M.G. Hauser et al., "Submillimeter Wavelength Survey of the Galactic Plane from l=-5 to l=+62: Structure and Energetics of the Inner Disk", Astrophys. J., **285**, 74, 1984.

[12] J.A.J. Skard et al., "The DIRBE Project Pipeline Software System", "Astronomical Data Analysis Software and Systems I" (eds: D.M. Worrall, C. Bimesderfer, and J. Barnes), Astron. Soc. Pac. Conf. Ser., **25**, 527, 1992.

[13] T.L. Murdock et al., "COBE/DIRBE Infrared Observations of the Ecliptic Poles", Bull. Am. Astron. Soc., **23**, 1313, 1992.

[14] C. Leinert, M. Hanner, and E. Pitz, "On the Spatial Distribution of Interplanetary Dust Near 1 AU", Astron. Astrophys., **63**, 183, 1978.

[15] C. Leinert, M. Hanner, I. Richter, and E. Pitz, "The Plane of Symmetry of Interplanetary Dust in the Inner Solar System", Astron. Astrophys., **82**, 328, 1980.

[16] R.H. Giese, B. Kneissel, and U. Rittich, "Three-Dimensional Models of the Zodiacal Dust Cloud: A Comparative Study", Icarus, **68**, 395, 1986.

[17] R.H. Giese and B. Kneissel, "Three-Dimensional Models of the Zodiacal Dust Cloud. II. Compatibility of Proposed Infrared Models", Icarus, **82**, 369, 1989.

[18] M.G. Hauser, "COBE/DIRBE Observations of Infrared Emission from Stars and Dust", "Back to the Galaxy" (eds: S.S. Holt and F. Verter), AIP Conf. Proc., to be published.

[19] W.T. Reach, "Zodiacal Emission. I. Dust Near the Earth's Orbit", Astrophys. J., **335**, 468, 1988.

[20] E.R. Duel and R.D. Wolstencroft, "A Physical Model for Thermal Emission from the Zodiacal Dust Cloud", Astron. Astrophys., **196**, 277, 1988.

[21] F.O. Clark et al., "The Out-of-Plane Distribution of the Zodiacal Dust Near the Earth", Astron. J., **105**, 976, 1993.

[22] S.F. Dermott, P.D. Nicholson, Y. Kim, and B. Wolven, "The Impact of IRAS on Asteroidal Science", "Comets to Cosmology" (ed: A. Lawrence), Lecture Notes in Physics, **297**, 3, 1988.

[23] S.F. Dermott and P.D. Nicholson, "IRAS Dust Bands and the Origin of the Zodiacal Cloud", Highlights in Astronomy, **8**, 259, 1989.

[24] M.V. Sykes, "Zodiacal Dust Bands: Their Relation to Asteroid Families", Icarus, **85**, 267, 1990.

[25] W.T. Reach, "Zodiacal Emission. III. Dust Near the Asteroid Belt", Astrophys. J., **392**, 289, 1992.

[26] J.L. Weiland et al., "COBE/Diffuse Infrared Background Experiment: Observations of Interplanetary Dust Bands", Bull. Am. Astron. Soc., **23**, 1313, 1992.

[27] G.B. Berriman et al., "Polarimetry with the Diffuse Infrared Background Experiment Aboard COBE", "Back to the Galaxy" (eds: S.S. Holt and F. Verter), AIP Conf. Proc., to be published.